PtRu nano-dandelions on thiolated carbon nanotubes: a new synthetic strategy for supported bimetallic core–shell clusters on the atomic scale†

Yong-Tae Kim,*[a] Hyunjoo Lee,[b] Hyoung-Juhn Kim[c] and Tae-Hoon Lim[c]

Core–shell PtRu clusters resembling dandelions were formed on thiolated carbon nanotubes by the difference in bond strength with surface thiol groups between Pt and Ru single atoms. The formation mechanism was clearly understood using a different release timing concept based on EXAFS and XPS analyses during heat treatment.

Bimetallic core–shell clusters are of great interest because of their unique properties and multi-functionality compared to monometallic clusters.[1] Many researchers have studied applications of bimetallic core–shell clusters to heterogeneous catalysis,[2] magnetic switching,[3] optical probes,[4] and fundamental structures.[5] Heterogeneous catalysis is one of the most interesting potential applications for bimetallic core–shell clusters because the catalysis reaction takes place only on the surface of the cluster. Hence, it could be an economic way to reduce the amount used of expensive noble metal by the substitution of the core part with inexpensive metal and shell coating. Also, the catalytic activity of bimetallic core–shell clusters with the same shell metal can be drastically changed with the core metal, which is called the ligand effect. Thereby, the catalytic activity in heterogeneous catalysis can be simply tuned with the change of core metal which brings about an alteration of electronic structure and adsorption strength.
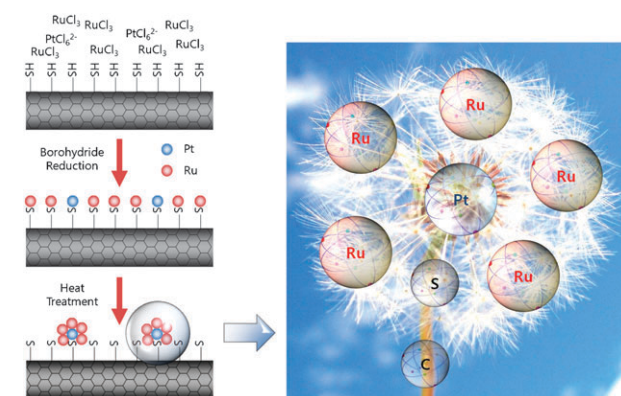
To date, various approaches have been suggested for bimetallic core–shell cluster formation; *e.g.*, successive two-step reduction,[6] underpotential deposition (UPD),[7] inter-matrix synthesis (IMS),[8] dendrimer template method,[9] spray pyrolysis,[10] redox-transmetalation process,[11] and Keggin ion-mediated synthesis.[12] Among these, the main approach employed in most of the studies was a successive two-step reduction; at first, the core part is formed by an appropriate reduction method, and then a precursor metal ion for the shell part is successively reduced onto the core metal. In this process, it is fairly difficult to synthesize the core–shell clusters on the the sub-10 nm scale, in addition to the problem of process complexity. Such complexity has been the main drawback to

applying the method to heterogeneous catalysts requiring a large surface area with small size.

Herein, we report a unique strategy for the formation of supported core–shell clusters in the shape of nano-dandelions on the atomic scale in which the core is a single Pt atom and the shells are several agglomerated Ru atoms. Such an interesting structure resulted from the difference of bond strengths with sulfur atoms in thiol groups between Pt and Ru single atoms which formed onto surface thiol groups of carbon nanotubes by borohydride reduction; the Ru–S bond is much weaker than the Pt–S bond. This brings about the faster release of Ru atoms from thiol groups than from Pt atoms during heat treatment; then, the drifting Ru atoms cover the Pt single atoms still linked to surface thiol groups and form a nano-dandelion structure. The main advantage of this unique synthetic strategy for core–shell clusters *versus* the conventional method is that it is possible to synthesize very small core–shell clusters below 1 nm in size. This feature enables us to apply core–shell clusters to heterogeneous catalysts, and to study the ligand effect on the atomic scale.

Scheme 1 shows the formation mechanism of a PtRu nano-dandelion based on the single atom to cluster (SAC) approach previously reported by the authors.[13] The experimental details are available in the electronic supplementary information.† Briefly, this unique approach is composed of three steps:

(1) Introduction of surface thiol groups on multi-walled carbon nanotubes, denoted by S-MWNTs.

(2) Formation of a single Pt and Ru atom monolayer onto a S-MWNT by borohydride reduction, denoted by PtRu-S-MWNT.

(3) Formation of PtRu core–shell clusters in the shape of dandelions on S-MWNTs by slight heat treatment at an appropriate temperature, wherein the release from surface

[a] School of Mechanical Engineering and Research Institute of Mechanical Technology, Pusan National University, Busan 609-735, Korea. E-mail: yongtae@pusan.ac.kr; Fax: (+82) 51 514 0685; Tel: (+82) 51 510 1012
[b] Department of Chemical and Biomolecular Engineering, Yonsei University, Seoul 120-749, Korea
[c] Fuel Cell Research Center, Korea Institute of Science and Technology, Seoul 136-791, Korea
† Electronic supplementary information (ESI) available: Experimental details, TEM images, XANES and extracted EXAFS signals in k-space for Pt L$_3$ and Ru K edge. See DOI: 10.1039/b920149a

Scheme 1 PtRu nano-dandelion formation mechanism based on SAC (Single Atom to Cluster) approach.

thiol groups of Ru atoms is possible, while release for Pt is impossible.

The first and second steps have been verified in our previous studies.[14] Notably, the metal single atoms in step 2 were of a closely reduced state rather than an ionic state of precursor, which was identified with the drastically decreased white line in XANES (X-ray Absorption Near Edge Structure) spectra and the binding energy shift of Pt 4f to higher energy in XPS (X-ray Photoelectron Spectroscopy), reflecting the final state effect. The heat treatment induced the Ru single atoms to be released from surface thiol groups because the heat treatment temperature was high enough to break a weak Ru–S bond due to a relatively low affinity between them. The released Ru atoms could drift on MWNT surfaces and agglomerate onto the Pt single atom seeds still linked to surface thiol groups with their strong Pt–S bond. These could form clusters having a unique structure in the shape of a dandelion on a S-MWNT, as shown in Scheme 1. This unique structure was revealed by EXAFS (Extended X-ray Absorption of Fine Structure) analysis with a synchrotron beam. As shown in Fig. 1, the changes of EXAFS radial distribution functions (RDFs) with heat treatment temperature for Pt L_3 and Ru K absorption edges are in striking contrast. For RDF from the Pt L_3 edge in Fig. 1(A), the main peak at about 1.9 Å, indicated by the blue arrow, corresponds to the first nearest neighbor (1NN) of the Pt–S bond having a coordination number of about 3. Since the single Pt atom is formed by linking to 3 sulfur atoms in surface thiol groups, only the peak corresponding to Pt–S is present without any peaks corresponding to the Pt–Pt bond in RDF. With the increase in heat treatment temperature, the main peak decreased slightly; however, a shoulder peak indicated by the red arrow increased at the right side of the main peak. This shoulder peak was revealed to correspond to the Pt–Ru bond with data fitting to the theoretical structure calculated by FEFF8 software. The increase of this peak, therefore, meant the gradual formation of a Pt–Ru bond; that is, Pt single atom core–Ru shell clusters (resembling dandelions) onto surface thiol groups like dandelion stems. The slight decrease of the Pt–S peak can be rationalized by some release of Pt single atoms occasionally having a weak bond, possibly due to a lower coordination number with sulfur atoms. On the other hand, the change of RDF obtained from the Ru K edge which reflects the surrounding atoms situation in view of the center Ru atom is perfectly different from that for the Pt L_3 edge, as shown in Fig. 1(B). In contrast to the absence of the peak corresponding to 1NN Pt–Pt in the RDF obtained from the Pt L_3 edge during heat treatment, the main peak corresponding to 1NN Ru–Ru including the smaller portion of Ru–Pt

Fig. 1 Radial distribution function (RDF) of EXAFS for (A) Pt L_3 and (B) Ru K absorption edge.

indicated by the orange-colored arrow rapidly increased with heat treatment temperature. This can be interpreted in terms of a different release timing concept: the Ru atoms can easily be released from the surface thiol groups and agglomerate with each other on Pt atom seeds which are still linked to the functional groups during heat treatment. Consequently, this change of RDFs during heat treatment provides direct evidence of PtRu core–shell structure formation on surface thiol groups in the shape of dandelions. Also, the peak indicated by the green arrow corresponding to the 1NN Ru–S bond rapidly vanished and changed into the peaks corresponding to 1NN Ru–O. This is because Ru atoms were first released from the thiol groups (the vanishing of 1NN Pt–S) and were easily oxidized during heat treatment. This phenomenon could also support the mechanism of PtRu core–shell structure formation. Some results on fine structure obtained by data fitting to our theoretical EXAFS model by using FEFF8 and Artemis are listed in Table 1, where the previously mentioned changes of RDFs are quantitatively demonstrated. To summarize the EXAFS results, it is clear that under an appropriate heat treatment temperature in which the Pt–S bond is not broken but the Ru–S bond should be broken, the drifting Ru atoms can agglomerate onto the Pt atom seeds linked to the surface thiol groups and form the unique dandelion structure.

The ligand effect, based on charge transfer in bimetallic clusters, can be identified using XPS studies. As shown in Fig. 2, there is a change of binding energy with heat treatment temperature. In Fig. 2(A), the binding energy (BE) for the Pt 4f core level is shifted considerably, to about 2.8 eV higher than bulk Pt (BE = 71.2 eV). This large shift resulted from the Pt single atom and can be elucidated with final state effect as one of quantum size effects which originates from the discrete electronic band structure with the decrease of particle size.[15] This result is consistent with our previous study on the

Table 1 Quantitative results on data fitting to theoretical model obtained from FEFF8

| Samples	1NN	N	R/Å	ΔE/eV	σ^2/Å^2
		Pt L_3			
PtRu-S-MWNT	Pt–S	3.427	2.125	2.721	0.002
HT (T_h = 473 K)	Pt–Pt	1.457	2.721	12.378	0.006
	Pt–Ru	2.378	2.708	7.253	0.005
	Pt–S	3.211	2.132	3.127	0.003
HT (T_h = 498 K)	Pt–Pt	1.576	2.735	12.587	0.006
	Pt–Ru	2.876	2.722	6.256	0.006
	Pt–S	2.745	2.158	2.985	0.004
HT (T_h = 523 K)	Pt–Pt	1.887	2.744	11.053	0.005
	Pt–Ru	4.289	2.731	3.587	0.006
	Pt–S	2.314	2.126	3.336	0.003
Samples	1NN	Ru K			
		N	R/Å	ΔE (eV)	σ^2 (Å^2)
PtRu-S-MWNT	Ru–S	1.376	2.248	3.875	0.005
HT (T_h = 473 K)	Ru–Ru	3.158	2.695	−3.235	0.001
	Ru–Pt	1.146	2.716	−2.845	0.004
	Ru–O	0.974	2.187	11.854	0.006
HT (T_h = 498 K)	Ru–Ru	3.257	2.701	−3.587	0.001
	Ru–Pt	1.189	2.720	4.852	0.004
	Ru–O	1.314	2.123	13.469	0.006
HT (T_h = 523 K)	Ru–Ru	4.037	2.712	−3.997	0.001
	Ru–Pt	1.535	2.723	−4.581	0.002
	Ru–O	1.571	2.095	−2.532	0.007
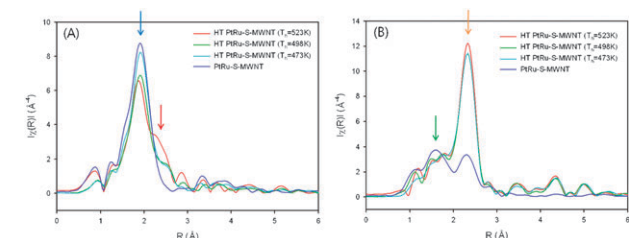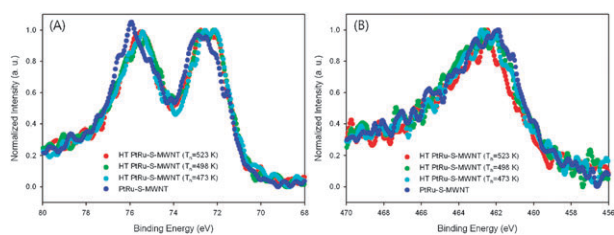
Fig. 2 XPS spectra for (A) Pt 4f and (B) Ru 3p core level.

dependence of Pt electronic structure on particle size based on the final state effect.[14] Before heat treatment, the Pt single atoms linked to surface thiol groups donate one electron to sulfur atoms to form a self-assembly between them, as follows:

$$RSH + M_n^0 \rightarrow RS^-M^+M_{n-1}^0 + \tfrac{1}{2}H_2$$

This electron donation, and the final state effect, leads to the considerable BE shift to higher energy from bulk.[16] However, the slight BE shift to lower energy after heat treatment is attributed to the Ru shell formation onto core Pt atoms in the shape of a dandelion, in which an electron from Ru can compensate the electron vacancy of the Pt side due to the electron donation of core Pt to sulfur atoms. Notably, the BE shift of the Ru 3p core level provided direct evidence of charge transfer to Pt as shown in Fig. 2(B). Indeed, Ru 3d, rather than 3p, is the electronic energy level showing the strongest intensity in photoelectron emission. However, we employed the Ru 3p orbital to show the BE shift by heat treatment temperature change, because the range of Ru 3d BE unfortunately overlapped with that of C 1s BE. As expected, the BE shift of Ru 3p to higher energy was observed, which reflected the charge transfer from Ru to Pt by PtRu core–shell structure formation after heat treatment. These BE shifts therefore strongly support the suggested formation mechanism of PtRu core–shell clusters in the shape of dandelions at the atomic scale.

Finally, we have tried to directly observe the size and morphology of PtRu nano-dandelion clusters with transmission electron microscopy (TEM). As shown in ESI Fig. 1,† it was difficult to clearly distinguish the clusters from MWNT supports owing to their extremely small size (below 1 nm). Furthermore, we failed to obtain the dandelion image with HRTEM, because the clusters agglomerated with each other during TEM observation by collision with accelerated electrons, as we reported previously.[13] (see ESI Fig. 2†) However, we firmly believe that the dandelion structure formation can be clearly proved with EXAFS analyses.

In conclusion, we have demonstrated the formation mechanism of a unique PtRu nano-dandelion structure. The difference in bond strength with the sulfur atom between Pt and Ru single atoms led to the different release timing of metal atoms from thiol groups during heat treatment; thus, the previously released Ru atoms could drift on the surface carbon nanotubes and cover the surface of single Pt atoms linked to thiol groups. This unique structure can be formed with not only Pt and Ru systems, but all atoms having different bond strengths with sulfur atoms which can bring about the different release time during heat treatment at an appropriate temperature.

Notes and references

1 (a) S. Sun, C. B. Murray, D. Weller, L. Folks and A. Moser, *Science*, 2000, **287**, 1989; (b) V. I. Klimov, A. A. Mikhailovsky, A. M. S. Xu, J. A. Holingsworth, C. A. Leatherdale, H. J. Eisler and M. G. Bawendi, *Science*, 2000, **290**, 314; (c) Q. Yuan, J. Zhuang and X. Wang, *Chem. Commun.*, 2009, 6613; (d) H. Miyamura, R. Matsubara and S. Kobayashi, *Chem. Commun.*, 2008, 2031.
2 (a) Y. Mizukoshi, T. Fujimoto, Y. Nagata, R. Oshima and Y. Maeda, *J. Phys. Chem. B*, 2000, **104**, 6028–6032; (b) S. U. Son, Y. Jang, J. Park, H. B. Na, H. M. Park, H. J. Yun, J. Lee and T. Hyeon, *J. Am. Chem. Soc.*, 2004, **126**, 5026; (c) S. Zhou, B. Varughese, B. Eichhorn, G. Jackson and K. McIlwrath, *Angew. Chem., Int. Ed.*, 2005, **44**, 4539.
3 (a) G. Rossi, A. Rapallo, C. Mottet, A. Fortunelli, F. Baletto and R. Ferrando, *Phys. Rev. Lett.*, 2004, **93**, 105503; (b) S. Rusponi, T. Cren, N. Weiss, M. Epple, P. Buluschek, L. Claude and H. Brune, *Nat. Mater.*, 2003, **2**, 546.
4 (a) A. Henglein, *J. Phys. Chem. B*, 2000, **104**, 2201; (b) K. Mallik, M. Mandal, N. Pradhan and T. Pal, *Nano Lett.*, 2001, **1**, 319.
5 (a) L. Cao, L. Tong, P. Diao, T. Zhu and Z. Liu, *Chem. Mater.*, 2004, **16**, 3239; (b) R. G. Sanedrin, D. G. Georganopoulou, S. Park and C. A. Mirkin, *Adv. Mater.*, 2005, **17**, 1027.
6 D. Ferrer, A. Torres-Castro, X. Gao, S. Sepulveda-Guzman, U. Ortiz-Mendez and M. Jose-Yacaman, *Nano Lett.*, 2007, **7**, 1701.
7 L. Wang, S. Guo, J. Zhai, X. Hu and S. Dong, *Electrochim. Acta*, 2008, **53**, 2776.
8 D. N. Muraviev, J. Macanas, P. Ruiz and M. Munoz, *Phys. Status Solidi A*, 2008, **205**, 1460.
9 M. R. Knecht, M. G. Weir, A. I. Frenkel and R. M. Crooks, *Chem. Mater.*, 2008, **20**, 1019.
10 K. C. Pingali, S. Deng and D. A. Rockstraw, *Chem. Eng. Commun.*, 2007, **194**, 780.
11 W. Lee, M. G. Kim, J. R. Choi, J. I. Park, S. J. Ko, S. J. Oh and J. Cheon, *J. Am. Chem. Soc.*, 2005, **127**, 16090.
12 S. Mandal, P. Selvakannan, R. Pasricha and M. Sastry, *J. Am. Chem. Soc.*, 2003, **125**, 8440.
13 Y.-T. Kim, K. Ohshima, K. Higashimine, T. Uruga, M. Takata, H. Suematsu and T. Mitani, *Angew. Chem., Int. Ed.*, 2006, **45**, 407.
14 Y.-T. Kim, T. Uruga and T. Mitani, *Adv. Mater.*, 2006, **18**, 2634.
15 G. K. Wertheim, S. B. DiCenzo and S. E. Youngquist, *Phys. Rev. Lett.*, 1983, **51**, 2310.
16 R. G. Nuzzo, B. R. Zegarski and L. H. Dubois, *J. Am. Chem. Soc.*, 1987, **109**, 733.